

# Validation of HDAC8 Inhibitors as Drug Discovery Starting Points to Treat Acute Kidney Injury

Published as part of the ACS Pharmacology & Translational Science special issue “Epigenetics 2022”.

Keith Long, Zoe Vaughn, Michael David McDaniels, Sipak Joyasawal, Aneta Przepiorski, Emily Parasky, Veronika Sander, David Close, Paul A. Johnston, Alan J. Davidson, Mark de Caestecker, Neil A. Hukriede,\* and Donna M. Hurny\*



Cite This: <https://doi.org/10.1021/acscptsci.1c00243>



Read Online

ACCESS |



Metrics & More



Article Recommendations



Supporting Information



**ABSTRACT:** Acute kidney injury (AKI), a sudden loss of kidney function, is a common and serious condition for which there are no approved specific therapies. While there are multiple approaches to treat the underlying causes of AKI, no targets have been clinically validated. Here, we assessed a series of potent, selective competitive inhibitors of histone deacetylase 8 (HDAC8), a promising therapeutic target in an AKI setting. Using biochemical assays, zebrafish AKI phenotypic assays, and human kidney organoid assays, we show that selective HDAC8 inhibitors can lead to efficacy in increasingly stringent models. One of these, PCI-34051, was efficacious in a rodent model of AKI, further supporting the potential for HDAC8 inhibitors and, in particular, this scaffold as a therapeutic approach to AKI.

**KEYWORDS:** acute kidney injury, histone deacetylase inhibitor, zebrafish, HDAC8, kidney organoids, PCI-34051

Acute kidney injury (AKI) is characterized by a sudden loss of kidney function. It affects millions of Americans every year, particularly those that are hospitalized.<sup>1</sup> Individuals at highest risk for developing AKI include diabetics, the elderly, those experiencing sepsis, and more recently, COVID-19 patients.<sup>2</sup> Mortality rates for AKI patients double within the first year, and costs of care more than triple. Furthermore, AKI is an independent risk factor for the development of chronic kidney disease (CKD),<sup>3</sup> which often results in patients requiring dialysis or transplantation. Despite the significant consequences of AKI, there are no approved therapies to treat the underlying disease, aside from supportive care.<sup>1</sup>

There are many causes of AKI, and its pathophysiology is not well understood, in part because physicians are reluctant to biopsy poorly functioning kidneys in AKI patients. However, recent efforts have led to the identification of potential therapeutic targets that fall into the general categories of anti-inflammatories, antioxidants, apoptosis inhibitors, hemodynamic modulators, metabolism modulators, compounds that modulate mitochondrial function, and repair agents.<sup>4</sup> Among these therapeutic targets, histone deacetylases (HDACs) have shown promise, with evidence of protective and pro-reparative effects of HDAC inhibitors in multiple experimental AKI

models.<sup>5,6</sup> For example, the nonselective HDAC inhibitor Trichostatin A (TSA) and the Class 1 selective inhibitor MS-275 show protective effects on renal injury and/or postinjury fibrosis in ischemia reperfusion-induced AKI (IRI-AKI) models.<sup>7</sup> However, there are also contradictory data that there may be a worsening of renal injury after IRI-AKI with the same molecules.<sup>8,9</sup> In addition, systemic toxicity of non-selective HDAC inhibitors raises concerns about their use in patients with AKI.<sup>6</sup> Given the positive evidence for HDAC inhibition as a therapeutic approach, recent focus has been on evaluating which HDAC subtype should be targeted in an AKI setting. Our efforts in this area stemmed from preliminary studies suggesting that selective modulation of HDAC8 provides a protective effect in zebrafish models of AKI. In addition, others have suggested inhibition of HDAC8 as a

Received: November 7, 2021

therapeutic approach based on effects on renal fibrosis after unilateral ureteric obstruction (UUO)<sup>10</sup> and renal protection in a cellular hypoxia model with HDAC8 inhibitors.<sup>11</sup> While there are multiple selective HDAC8 inhibitors known, a study of their activity in an AKI setting has not been performed.

To validate HDAC8 inhibitors as potential starting points for drug discovery, we synthesized and tested a series of known potent, selective HDAC8 competitive inhibitors with distinct structures. We reasoned that by evaluating inhibitors from multiple scaffolds in increasingly stringent assays, we would reduce the possibility of scaffold-specific effects compromising our conclusions. We also synthesized a small set of novel analogs within one of the series with a goal of identifying HDAC8 inhibitors that were predicted to have improved properties, particularly solubility. A zebrafish AKI (zfAKI) model was used to prioritize compounds for more extensive evaluation in efficacy studies in human kidney organoid assays. Finally, we report data on the effects of the selective HDAC8 inhibitor PCI-34051 in a mouse model of AKI. Together, this work provides further support for HDAC8 inhibition as a therapeutic target for AKI and interrogates which HDAC8 scaffolds may be most promising as starting points for medicinal chemistry optimization.

From the potent and selective competitive HDAC8 inhibitors reported in the literature,<sup>12,13</sup> we chose to evaluate the hydroxamic acid-containing PCI-34051<sup>14</sup> as well as a series of tetrahydroisoquinoline (THIQ) hydroxamic acids<sup>15</sup> (2–13) that, depending on structure, exhibit a range of HDAC8 selectivity profiles (Figure 1). This series offered the



**Figure 1.** Inhibitor PCI-34051, general structure of tetrahydroisoquinolines (THIQs), and isoindolyl amide 1.

opportunity to evaluate scaffold-specific effects vs HDAC8 inhibitory effects. To account for the potential of hydroxamic acids exerting off-target effects,<sup>16</sup> as reported for PCI-34051,<sup>17</sup> we also synthesized and evaluated the potent and selective HDAC8 inhibitor isoindolyl amide 1 (Figure 1).<sup>18</sup> The pan-HDAC inhibitors SAHA (suberoylanilide hydroxamic acid; Vorinostat) and Belinostat were also evaluated.<sup>19</sup>

We first confirmed HDAC8 activity in a commercially available biochemical assay that relied on a fluorescent readout.<sup>20</sup> To prioritize compounds for more extensive (and labor intensive) organoid and *in vivo* studies, we utilized a phenotypic zfAKI assay.<sup>21</sup> Briefly, injection of zebrafish larvae with nephrotoxic levels of gentamicin results in proximal tubule injury and eventually lethality ~3–7 days postinjection (dpi).<sup>22</sup> In this testing paradigm, when injury is established at 2 dpi, zf larvae are placed in media containing test compound at 4  $\mu$ M, and survival is assessed on days 3–7 postinjection. Protective compounds extend survival as measured by the Kaplan–Meier estimator (Figure S1).<sup>23</sup>

In a previous study, we characterized the common properties of 700 small molecules that exhibit biological effects in zf assays.<sup>24</sup> This work, modeled after the well-known parameters used to guide the design of orally bioavailable drugs,<sup>25</sup> was aimed at providing data in terms of molecular characteristics

(e.g., clogP, total polar surface area, H-bond donor and acceptor count, etc.) that represent 90% of zf-active small molecules. These calculated properties were not segregated with respect to various barriers that would preclude zf activity (e.g., impermeability, metabolic instability, and sequestration) and, therefore, reflect the constellation of characteristics that are necessary for a compound to exhibit effects in zf phenotypic assays. Importantly, the properties of all the tested compounds herein fall within the 95th percentile of zf-active small molecules, supporting the probability that there are no obvious barriers to their *in vivo* efficacy in the zfAKI assay (Table S1).

Confirming the literature reports, in our hands, PCI-34051, THIQs 2 (R = biphenyl,  $x = 2$ ) and 3 (R = *p*-methoxyphenyl,  $x = 2$ ), and isoindolyl amide 1 exhibited potent HDAC8 inhibitory activity (Tables 1 and S2; reported selectivity vs other HDACs also included). In the zfAKI assay, PCI-34051,

**Table 1.** Activity of Known HDAC8 Inhibitors in Biochemical and zf AKI Assays and Literature Selectivity Data

Compound	HDAC8 IC <sub>50</sub> $\mu$ M (sd)*	Zf AKI Efficacy $\mu$ M #	HDAC Selectivity <sup>†</sup> HDACX/HDAC8 vs. HDACs
PCI-34051	0.12 (0.05)	4	>200 vs. 1,2,3,6,10 <sup>17</sup>
1	0.15 (0.02)	4	>15 vs. 1,2,6 <sup>18</sup>
[rac]-2	0.42 (0.10)	4	>100 vs. 1,2,3,6 <sup>15</sup>
(+)-2	0.43 (0.05)	4	>20 vs. 1,2,3,6 <sup>^</sup>
(-)-2	31.2 (NC)	NE	NC
3	2.4 (0.38)	4	>200 vs. 1,2,3,6 <sup>15</sup>
4	>40	NE	1 vs. 6 $\geq$ 5 vs. 1,2,3 <sup>15</sup>
5	10.8 (3.7)	NE	>6 vs. 1,2,3,6 <sup>15</sup>
6	9.3 (3.6)	NE	>50 vs. 1,2,3,6 <sup>15</sup>
7	>40	NE	>4-fold vs. 1,2,3,6 <sup>15</sup>
SAHA	6.1 (0.92)	4	<0.10 vs. 1-4,6,7,9 <sup>17,19</sup>
Belinostat	1.0 (0.12)	4	<0.6 vs. 1-4,6,7,9 <sup>19</sup>

\*  $n \geq 2$ . #  $p \leq 0.05$ ,  $n \geq 3$ . <sup>†</sup> Selectivity values based on literature cited except where noted by <sup>^</sup>. sd = standard deviation. NE = not effective. NC = not calculated.

compound **1**, and racemic compounds **2** and **3** were efficacious in extending survival when dosed at 4  $\mu\text{M}$ .

To further explore these findings, we separated the enantiomers of **2**. The (+)-enantiomer was considerably ( $\sim 100$ -fold) more potent in the biochemical HDAC8 assay ( $\text{IC}_{50} = 0.43 \mu\text{M}$ ) than (–)-**2** ( $\text{IC}_{50} = 31.2 \mu\text{M}$ ) (Tables 1 and S2). Selectivity vs HDACs 1, 2, 3, and 6 was also maintained for (+)-**2**. Consistent with these results, the eutomer was effective in the zfAKI assay at 4  $\mu\text{M}$ , while the distomer was inactive. These data, in particular the consistent separation of activity between the enantiomers of compound **2**, support our hypothesis that potent HDAC8 activity can lead to phenotypic zfAKI efficacy and is not scaffold-related.

Within the THIQ series, we evaluated additional analogs chosen for their specific potency and/or selectivity profiles (compounds 4–7). We reasoned that by testing compounds within the same scaffold with very similar physical properties (Table S1), we would minimize other variables, distinct from biochemical potency, that might contribute to differential effects in the zf phenotypic assay. We confirmed HDAC8  $\text{IC}_{50}$ 's internally (Tables 1 and S2); in general, the trends for potency were similar to those reported,<sup>15</sup> albeit, under our assay conditions, potencies were lower. None of the compounds showed improvement in survival in the zfAKI assay when tested at 4  $\mu\text{M}$ . The lack of zfAKI activity for analogs **4** and **7** was expected given their lack of HDAC8 biochemical activity and allows us to conclude that off-target, scaffold-derived effects do not contribute to zf efficacy. However, based on their activity in the biochemical assay, we expected to see some modest effects for compound **5** or **6**. It is possible there is a threshold for potency, and the  $\sim 4$ -fold lower potency of these THIQs was not sufficient for zf efficacy at 4  $\mu\text{M}$ , a concentration selected based on the effects of PCI-34051. The pan-HDAC inhibitors SAHA and Belinostat, with modest HDAC8 potencies ( $\text{IC}_{50} = 6 \mu\text{M}$  and  $1.4 \mu\text{M}$ , respectively) and potent activities at other HDACs, were effective in the zfAKI assay at 4  $\mu\text{M}$ . One hypothesis is that inhibition of other HDACs contributes to the efficacy observed for SAHA and Belinostat, a hypothesis supported by the lack of efficacy of compound **6** with similar potency vs HDAC8 but no activity at other HDACs.

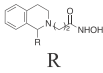
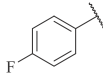
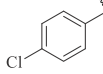
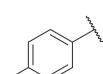
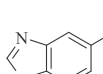
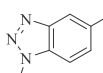
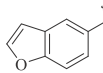
Some broad conclusions can be drawn from these data. First, highly potent ( $\text{IC}_{50} < 500 \text{ nM}$ ) and selective HDAC8 inhibitors of diverse scaffolds exhibit efficacy in the zfAKI assay, further supporting this therapeutic approach to AKI. Second, the zfAKI assay appears to be valuable for high potency compounds, but for those with modest biochemical potency (e.g., mid- $\mu\text{M}$ ), the correlation is less direct. Efficacy or lack of efficacy of compounds such as these may be the result of additional factors (e.g., localization, metabolism, etc.) that can be overcome by more potent analogs. Finally, pan-HDAC inhibition will also result in efficacy in this model, a result consistent with data from studies in proximal tubular cells.<sup>26</sup>

With the promising data for compounds (+)-**2** and **3** in the zfAKI assay, we prepared a small number of novel analogs that were designed to maintain HDAC8 potency and selectivity but exhibit improvements in physical and pharmaceutical properties. For example, compound **2** had poor solubility in our hands, requiring a modified formulation in the zfAKI assay. We were also concerned about the potential for metabolic instability due to the presence of the aryl methyl ether in compound **3**. Specific analogs designed to address these issues

included the halogenated phenyl analogs **8** and **9** and tolyl analog **10**. We incorporated heterocycles such as benzimidazole (**11**), benzotriazole (**12**), and benzofuran (**13**) in an effort to improve solubility (Table S1) and mimic the structural features of the biphenyl and *para*-methoxy phenyl groups found in actives **2** and **3**. Synthesis of these compounds was based on reported methods.<sup>15</sup>

Results of biochemical and zfAKI assays for these novel analogs are shown in Tables 2 and S2. Of the new analogs 8–

**Table 2. Activity of Novel THIQs in Biochemical and zf AKI Assays**

Compound		HDAC8 $\text{IC}_{50}$ $\mu\text{M}$ (sd)*	Zf AKI Efficacy $\text{EC}_{50}$ $\mu\text{M}$ <sup>#</sup>	HDAC Selectivity % inhibition @10 $\mu\text{M}$
8		8.1 (3.4)	NE	<25% @ HDAC 1,2,3,6
9		3.3 (1.1)	NE	<25% @ HDAC 1,2,3,6
10		4.6 (1.6)	NE	<25% @ HDAC 1,2,3,6
11		7.5 (3.2)	NE	<25% @ HDAC 1,2,3; $\sim 40\%$ @ HDAC6
12		15.4 (7.3)	4	<25% @ HDAC 1,2,3,6
13		4.6 (2.1)	4	<25% @HDAC 1,2,3,6

\*  $n \geq 2$ . <sup>#</sup>  $p \leq 0.05$ .  $n \geq 3$ . sd = standard deviation. NE = not effective.

**13**, all exhibited HDAC8 inhibition in the micromolar range, with analogs **9**, **10**, and **13** being the most potent ( $\text{IC}_{50} = 3.3$ , 4.6, and 4.6  $\mu\text{M}$ , respectively) and in the same range as *p*-methoxy analog **3**. Selectivity was evaluated at 10  $\mu\text{M}$ , and all except **11** showed essentially no effects at HDAC 1, 2, 3, or 6. The imidazole **11** was modestly active at HDAC6, with  $\sim 40\%$  inhibition at 10  $\mu\text{M}$ . All compounds were evaluated in the zfAKI assay, and of these, surprisingly, the most potent compound **9** was inactive, despite potency and physical properties that were very similar to the active compound **3**; also unexpected was the efficacy of the benzotriazole **12**, which exhibits only weak HDAC8 ( $\text{IC}_{50} = 15.4 \mu\text{M}$ ) activity, a similar profile to the zf inactive compound **6** ( $\text{IC}_{50} = 9.3 \mu\text{M}$ ,  $>50$ -fold selective). These data raise the question of whether this THIQ scaffold (vs the PCI-34051 or compound **1** scaffold) is a robust starting point for medicinal chemistry optimization.

Based on their robust activity in the zfAKI assay and their solubility in our standard assay media (vs compound 2, which required modification of the assay protocol), we evaluated PCI-34051, compound 1, and compound 3 in a human kidney organoid assay that we believe recapitulates some of the fibrotic processes that occur after AKI and are presumed to be initiating events for the development of CKD. In this assay, day 14 organoids were treated with 12.5  $\mu\text{M}$  hemin for 2 days to induce reactive oxygen species (ROS) and inflammatory events<sup>27</sup> and then treated with test compounds at 5, 1, 0.2, and 0.04  $\mu\text{M}$  for 7 days. Fibrosis was measured by visualization based on collagen hybridizing peptide (CHP).<sup>28</sup> Of the three, PCI-34051 showed significant reduction of collagen deposition at all concentrations (minimal efficacious dose  $\leq 0.04 \mu\text{M}$ ), but effects were most robust at 1  $\mu\text{M}$  (Figure 2A and B). Compound 1 at all doses showed a general trend of decreased CHP staining compared to the hemin-injured control; however, none were statistically significant (Figure 2C). Compound 3 showed no effect at any dose (Figure S2).

We also tested the effects of PCI-34051 and compound 1 on immortalized human proximal tubule cells (RPTEC/TERT1) injured with the anticancer agent cisplatin, a cause of AKI clinically.<sup>29</sup> Briefly, RPTECs were synchronized and then treated with 15  $\mu\text{M}$  cisplatin for 48 h, followed by 10  $\mu\text{M}$  PCI-34051 or compound 1 in fresh medium for an additional 48 h. Expression of inflammatory marker genes was measured by quantitative RT-PCR (Q-RT-PCR). Robust induction of the pro-inflammatory cytokines *TNFA*, *CXCL1* (Figure 3), and *CXCL5*, *IL6*, *CXCL8/IL8*, *CCL2*, and the proteinase inhibitor and AKI biomarker *SERPINE1* was observed in cisplatin-treated cells (Figure S3). Treatment with PCI-34051 and compound 1 significantly reduced the upregulation of these genes. Neither compound had an effect on markers in uninjured cells, except for *CCL2*, which was induced 4–5-fold. Overall, these results are consistent with HDAC8 inhibition having an anti-inflammatory effect in the setting of cisplatin-induced injury and support the potential of both scaffolds.

Given the promising activity of PCI-34051 in both the organoid and proximal tubule cell models, as well as documented selectivity vs HDACs 1–3 and 6 in a cellular environment,<sup>14,30</sup> we explored its effects in a mouse AKI model that we developed in which an initial AKI event progresses to CKD (unilateral IRI (ischemia reperfusion-induced) followed by delayed contralateral nephrectomy; DN-IRI).<sup>31</sup> A pharmacokinetic (PK) study in CD1 mice (Table 3, Figure S4) showed measurable levels of the compound up to 24 h after doses of both 10.4 mg/kg and 52 mg/kg ip and, in general, dose-dependent exposure.

Based on the PK data, as well as published data indicating that daily treatment with PCI-34051 at 20 mg/kg is effective in reducing renal fibrosis in a mouse UUO model,<sup>10</sup> we dosed mice at 10 and 50 mg/kg ip for 7 days (Figure 4A). Renal functional recovery was evaluated by serial measurement of blood urea nitrogen (BUN) and transdermal glomerular filtration rate (GFR) 28 days after the initial injury by measuring cutaneous fluorescence decay of IV injected FITC-sinistrin, as described previously.<sup>32</sup> Renal fibrosis was assessed by quantifying renal staining with Sirius red and Q-RT-PCR for renal expression of the fibrosis markers *Collagen 1a1* (*Colla1*) and *LoxL2* at 28 days, as described.<sup>33</sup> There was no difference in survival between groups (Figure S5A). BUN levels were reduced in both treatment groups 9 days after

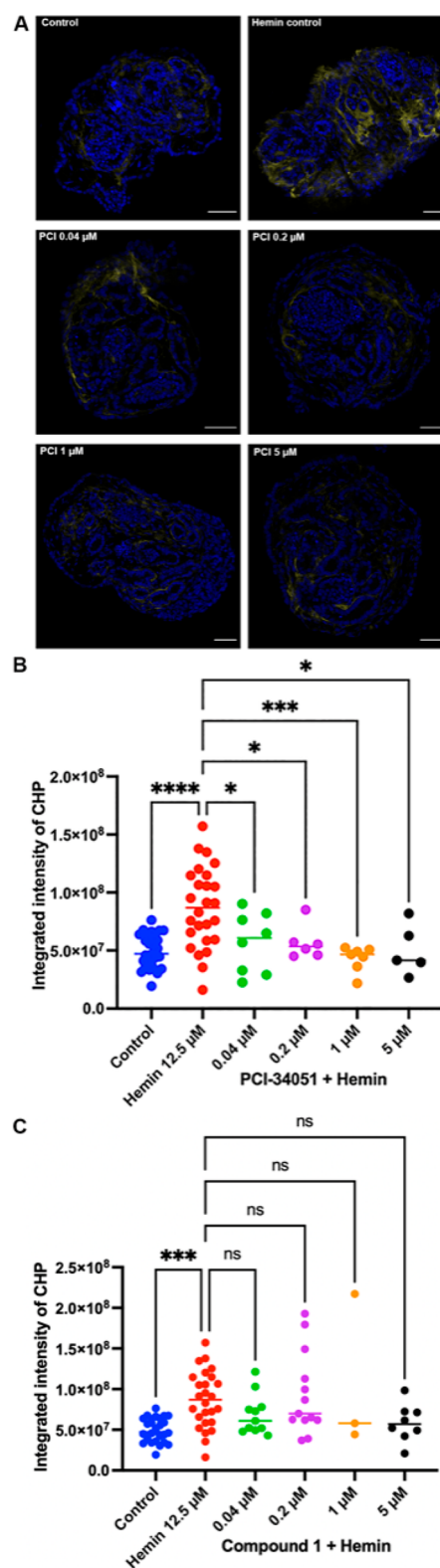


**Figure 2.** Human kidney organoids treated with HDAC8 inhibitors. (A) PCI-34051 at 5, 1, 0.2, and 0.04  $\mu\text{M}$ . Immunofluorescence of day 23 organoid sections stained with CHP (yellow) and nuclei (DAPI; blue). Scale bar = 100  $\mu\text{m}$ . (B) Quantification of CHP staining. Each data point represents the integrated intensity of CHP of an organoid section. \* $p < 0.05$ . \*\*\* $p < 0.001$ . \*\*\*\* $p < 0.0001$ . (C) Compound 1 at 5, 1, 0.2, and 0.04  $\mu\text{M}$  quantification of CHP staining. Each data point represents the integrated intensity of CHP of an organoid section. ns = not significant. \*\*\* $p < 0.001$ . One way ANOVA.

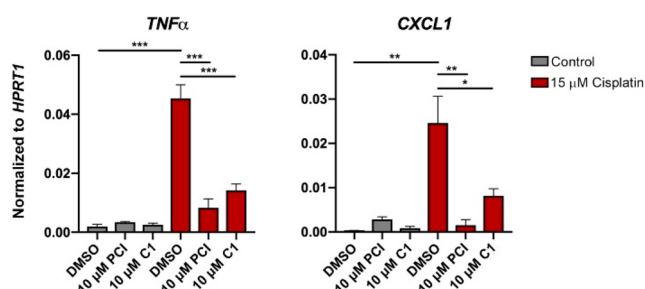


**Figure 3.** PCI-34051 and compound 1 reduce expression of inflammatory cytokines in cisplatin-treated human proximal tubule cells. Q-RT-PCR analyses of untreated and cisplatin-treated RPTECs  $\pm$  DMSO, PCI-34051, or compound 1 (C1). Data points are mean  $\pm$  SD. \* $p < 0.05$ . \*\* $p < 0.01$ . \*\*\* $p < 0.001$ . One way ANOVA.

**Table 3.** PK Parameters for PCI-34051

IP dose (mg/kg)	$T_{max}$ (h)	$C_{max}$ (ng/mL)	$AUC_{last}$ (h-ng/mL)	$AUC_{inf}$ (h-ng/mL)
10.4	0.25	3808	1851	1954
52	0.08	6157	6680	7636

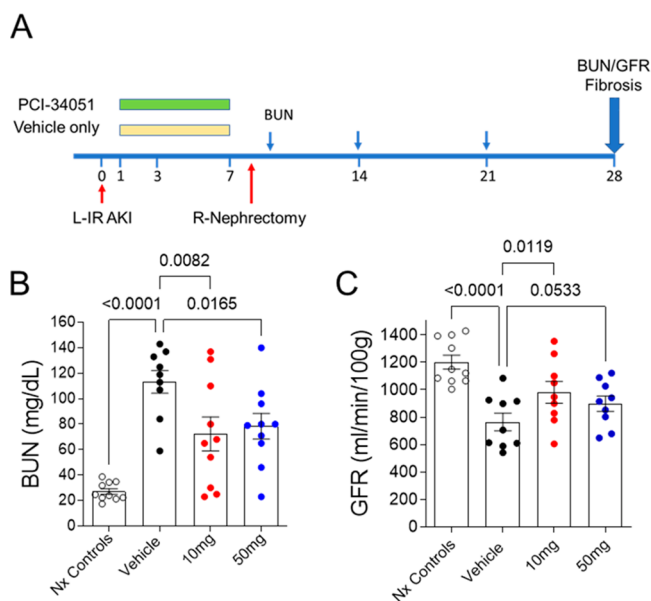


**Figure 4.** Effects of PCI-34051 at 10 and 50 mg/kg in the DN-IR AKI model. (A) Schematic of the DN-IR AKI study and treatment regimens. (B) Levels of BUN 9 days after L-IRI. (C) Transdermal GFR levels 27 days after IRI-AKI. Individual data points with mean  $\pm$  SEM shown. One way ANOVA was used to compare vehicle Nx control and treatment groups after injury ( $p \leq 0.001$  for all studies).  $p$  values shown were adjusted for multiple between group comparisons with false discovery rates of  $p < 0.05$ .

injury (Figure 4B) but equalized between groups over time (Figure S5B). Transdermal GFR, which is a more accurate indicator of mild renal impairment than BUN,<sup>33</sup> was significantly increased in mice treated with 10 mg/kg PCI-34051 at 28 days; tGFR was also increased in mice treated with 50 mg/kg PCI-34051 27 days after IRI, but these changes failed to reach statistical significance at the accepted  $p < 0.05$  level when compared with vehicle control mice ( $p = 0.053$ ), although the effects were trending in the same direction (Figure 4C). There was no significant reduction in renal fibrosis as determined by Sirius red staining, but mRNA

markers of renal fibrosis were reduced in mice treated with PCI-34051 (Figure S6).

In conclusion, we show that selective HDAC8 inhibitors representing multiple scaffolds (indole hydroxamic acid, THIQ, and indolylamide) can exhibit efficacy in a zf model of AKI, further strengthening and validating this therapeutic approach. Furthermore, applying a stringent compound progression strategy, including biochemical data and zf phenotypic efficacy, we showed that some of these analogs also exhibit efficacy in human kidney organoid models. The most robust effects were observed for PCI-34051, and this translated into efficacy in a rodent model of AKI. Our data supports that selective HDAC8 inhibitors, and in particular the indole hydroxamic acid scaffold, have the potential to be useful starting points for medicinal chemistry optimization and AKI drug discovery.

## METHODS

Compounds used in this study were prepared as described in the Supporting Information and determined to be >95% pure via either LC/MS or HPLC analysis. All novel final products were fully characterized (<sup>1</sup>H NMR, <sup>13</sup>C NMR, and MS). Known final products prepared via a different method than reported in the literature were characterized by <sup>1</sup>H NMR, <sup>13</sup>C NMR, and MS.

**HDAC8 Assay.** HDAC8 biochemical assays were conducted according to the manufacturer's instructions using the BPS Bioscience (San Diego, CA) HDAC8 Fluorogenic Assay Kit #50068, which contains HDAC8 enzyme, HDAC fluorogenic substrate, HDAC developer (2 $\times$ ), and HDAC assay buffer. The reactions were conducted in 384-well polystyrene nonbinding flat bottom microplates (Cat. # 781900) obtained from Greiner Bio-One (Monroe, NC). A master mix of 15  $\mu$ L containing HDAC substrate, bovine serum albumin (BSA), and HDAC assay buffer was dispensed into the wells of the microtiter assay plates. Compound wells received 5  $\mu$ L of a 5 $\times$  compound mixture diluted in HDAC assay buffer + 5% DMSO. Maximum (MAX) and no enzyme blank control wells received 5  $\mu$ L of HDAC assay buffer + 5% DMSO. Minimum (MIN) control wells received 5  $\mu$ L of 5 times PCI-34051 (10  $\mu$ M final) control inhibitor in HDAC assay buffer + 5% DMSO. Assay plates were pre-read for relative fluorescence intensity units (RFUs) at excitation 350 nm and emission 455 nm (Ex350/Em455) using a SpectraMax M5e (Molecular Devices, LLC, Sunnyvale, CA) multimode plate reader prior to the addition of HDAC8 enzyme to detect autofluorescent compounds which may interfere with the assay detection format. Reactions were initiated with the addition of 5  $\mu$ L of 5 times HDAC8 enzyme. Blank no enzyme control wells received 5  $\mu$ L of HDAC assay buffer. The final reaction volume was 25  $\mu$ L. Reactions were incubated at 37  $^{\circ}$ C for 30 min and then 25  $\mu$ L of HDAC developer (2 $\times$ ) was added to each well and assay plates were incubated at room temperature for 15 min before the RFUs (Ex350/Em455) were measured using a SpectraMax M5e multimode plate reader. Final HDAC8 assay conditions: HDAC8 enzyme 10 ng/well, HDAC substrate 2  $\mu$ M, BSA 0.1 mg/mL, DMSO 1%, MIN control compound PCI-34051 10  $\mu$ M, test compounds 2 nM – 40  $\mu$ M. To analyze the data, the mean RFUs of the blank no enzyme control wells were subtracted from the RFUs for the maximum and minimum control and test compound wells. The normalized percent inhibition (% inhibition) of each well was then calculated using the equation % Inhibition = (Mean

MAX RFUs – test sample RFUs)/(Mean MAX – Mean MIN RFUs) × 100. MAX, MIN, & no-enzyme BLANK control wells.  $n = 12–16$ . For test compounds, at least  $n = 2$  for each concentration.

**HDACs 1, 2, 3, and 6.** Selectivity assays, run by Reaction Biology,<sup>32</sup> relied on a peptide-based fluorogenic assay. Compounds were assessed at a single concentration of 10  $\mu\text{M}$  ( $n = 2$ ). The substrate for HDACs 1, 2, 3, and 6 was based on p53 residues 379–382 (RHKK(Ac)AMC). Percent inhibition was calculated relative to DMSO controls. Trichostatin A (TSA) was used as a positive reference compound.

**Zebrafish Assays.** Studies were approved by the University of Pittsburgh IACUC. Zebrafish were maintained as described,<sup>34</sup> and embryos from Pitt AB wildtype were used. Zebrafish larvae were injected with a single dose of gentamicin at 3 days post fertilization (dpf) with 7 ng of gentamicin as previously described.<sup>21</sup> Prior to the gentamicin injection, 3 dpf zebrafish larvae were anesthetized in 0.2% tricaine/E3 medium (5 mM NaCl, 0.33 mM CaCl<sub>2</sub>, 0.33 mM MgSO<sub>4</sub>, and 0.17 mM KCl). Glass capillaries were pulled to produce microneedles and were aspirated with 10  $\mu\text{L}$  of 7 ng/nL gentamicin solution diluted with filtered saline solution (Aspen Veterinary Resources, Cat No. 17861615). The larvae were injected with 1 nL of gentamicin solution, delivered via the common cardinal vein. After injection, larvae were incubated in 50  $\mu\text{g}/\text{mL}$  penicillin/streptomycin diluted in E3 medium. Test compounds were diluted in E3 medium containing 0.5% DMSO, except for [rac]-2, (+)-2, and (–)-2, which were diluted in Danieau's solution instead of E3. Larvae were treated with either DMSO, UPHD25, or test compounds (4  $\mu\text{M}$ ) from 2 days postinjection.

**Statistical Analysis.** Data were analyzed as compounds that extend survival as measured by the Kaplan–Meier estimator.<sup>21</sup> UPHD25 (HDAC inhibitor previously shown to be protective in kidney injury<sup>35</sup>) was used as a positive control and was statistically significant in all survival assays.

**Organoid Assays.** All work was carried out with the approval of IRB approval STUDY19020238 and biosafety approval IBC201600244. iPSCs were maintained on 10 cm cell culture dishes coated with Geltrex (Thermo Fisher) and mTeSR1 (Stemcell Technologies) medium. All experiments were performed with the MANZ-2-2 iPSC line, generated in the Davidson laboratory.<sup>36</sup> Kidney organoid assays were performed as described previously.<sup>33,37</sup> Briefly after Dispase treatment iPSC clusters were suspended in medium composed of TeSR-E5 (Stemcell Technologies), 0.1% ITS-X, 1% CD lipid concentrate (Gibco), 0.25% polyvinyl alcohol, 1% penicillin/streptomycin (Gibco), and 2.5  $\mu\text{g}/\text{mL}$  Plasmocin. On day 3 of the assay, embryoid bodies were transferred to the Stage II medium consisting of DMEM-low glucose, 10% KOSR (Thermo Fisher), 1% nonessential amino acids, 1% penicillin/streptomycin, 1% HEPES, 1% GlutaMAX, 0.25% polyvinyl alcohol, and 2.5 mg/mL Plasmocin. Hemin was made up in 0.1 M NaOH. Day 14 organoids were washed thrice with DMEM-low glucose before being placed into protein-free medium (1:1 ratio of DMEM-low glucose and Hams F-12 nutrient mixture), 1% HEPES, 1% penicillin/streptomycin (Gibco), and 2.5  $\mu\text{g}/\text{mL}$  Plasmocin containing Hemin in a 6-well ultralow attachment plate. The hemin concentration was at 12.5  $\mu\text{M}$ . The control well contained an equivalent volume of 0.1 M NaOH as a vehicle control. All treatments were maintained for 48 h.

Kidney organoids at day 16 post hemin treatment were washed 3× with Stage II medium. For compound treatment Stage II medium was supplemented with 0.3% DMSO. A 2× solution of compound was prepared in Stage II-DMSO, and a calculated amount was added to each well to make up 1× stock in a 3 mL volume, per well of a 6-well ULA plate. The plates were maintained on the magnetic stirrer at 25% power and 120 revolutions until day 23. Deparaffinized sections of kidney organoids were washed with DPBS. A working solution of CHP was first heated for 5 min at 80 °C, cooled on ice immediately, and distributed onto each section. Sections were stained overnight at 4 °C in a humidified chamber. The next day, sections were washed twice, and nuclei were stained with DAPI and mounted before imaging on a Zeiss LSM700 instrument. All images were taken with the same settings and analyzed using Fiji software. Statistical significance was tested with one-way ANOVA with Dunnett's multiple comparisons test in GraphPad Prism 9 software.

**PK Studies.** PK studies on PCI-34051 were performed at SAI Life Sciences Ltd., Pune, India, using male BALB/c mice following a single intraperitoneal dose of PCI-34051 in 5% NMP, 5% Solutol HS, 30% PEG-400, and 60% normal saline at 10.4 and 52 mg/kg. Blood samples (approximately 120  $\mu\text{L}$ ) were collected from retro-orbital plexus of three mice predose and at 0.08, 0.25, 0.5, 1, 2, 4, 8, and 24 h. Samples were collected into labeled microtubes, containing 20% K<sub>2</sub>EDTA as anticoagulant. Immediately, aliquots (50  $\mu\text{L}$ ) of blood were hemolyzed with an equal volume of water (50  $\mu\text{L}$ ) and quenched with three volumes (150  $\mu\text{L}$ ) of acetonitrile (IS containing acetonitrile) and samples were stored below –70 °C until bioanalysis. This study was performed with approval of Institutional Animal Ethics Committee (IAEC) in accordance with requirements of the Committee for the Purpose of Control and Supervision of Experiments on Animals, India. All samples were processed for analysis by protein precipitation using acetonitrile and analyzed with the fit for purpose LC/MS/MS method. PK parameters were calculated using the noncompartmental analysis tool of Phoenix WinNonlin (Version 7.0). Maximum concentration ( $C_{\text{max}}$ ) and time to reach maximum concentration ( $T_{\text{max}}$ ) were taken from the observed values. The areas under the concentration time curve ( $\text{AUC}_{\text{last}}$  and  $\text{AUC}_{\text{inf}}$ ) and elimination half-life were calculated by the linear trapezoidal rule.

**Proximal Tubule Cell Assay.** Human immortalized renal proximal tubule epithelial cells (RPTEC/TERT1; ATCC CRL-4031) were maintained in renal epithelial cell growth medium (REGM; Lonza Bioscience). Cells were synchronized by double thymidine block and then treated with 15  $\mu\text{M}$  cisplatin (Sigma) for 48 h, followed by 10  $\mu\text{M}$  PCI-34051 or compound 1 in fresh REGM for an additional 48 h. RNA isolation (GENEZol TriRNA Pure Kit) and cDNA synthesis (SuperScript IV VILO Master Mix; Invitrogen) were carried out, and expression levels were measured on a QuantStudio 6 Flex Real-Time PCR system, using the following primers: *CCL2* fwd, CAGCCAGATGCAATCAATGCC; rev, TGGAA-TCTGAACCCACTTCT; *CXCL1* fwd, GCGCCAAAC-CGAAGTCATA; rev, ATGGGGGATGCAGGATTGAG; *CXCL5* fwd, CAGACCACGCAAGGAGTTCATC; rev, TTCCTTCCCGTTCTTCAGGGAG; *HPRT1* fwd, CATTATGCTGAGGATTTGGAAAGG; rev, CTTGAGCACA-CAGGGGCTACA; *IL6* fwd, AGACCTTCCACTCAC-TCTAGG; rev, TTCTGCCAGTGCCTCTTTGCTG; *IL8* (*CXCL8*) fwd, GAGAGTGATTGAGAGTGGACCAC; rev,

CACAACCCTCTGCACCCAGTTT; *SERPINE1* fwd, CTCATCAGCCACTGGAAAGGCA; rev, GACTCGTGAA-GTCAGCCTGAAAC; *TNF $\alpha$*  fwd, CTCTTCTGCCTGCTG-CACCTTTG; rev, ATGGGCTACAGGCTTGTCACTC. Measurements were performed in triplicate. Statistical analysis was performed using one-way ANOVA in Prism.

**Ischemia Reperfusion-Induced Acute Kidney Injury (IRI-AKI).** Surgeries were performed on a water bath-heated platform at 38 °C on 10- to 12-week-old male BALB/c mice purchased from Charles River Laboratories. To induce IRI-AKI, mice underwent left renal pedicle clamping for 30–31 min, and delayed contralateral nephrectomy was performed after 8 days, as described.<sup>33</sup> Separate cohorts of mice underwent contralateral nephrectomy alone for comparison. Mouse numbers and survival after the surgeries are documented over time in Figure S5A, and mice were euthanized for tissue harvesting and terminal blood draw 28 days after the initiating injury. Blood urea nitrogen (BUN) was determined in duplicate samples using a colorimetric assay kit (Infinity Urea, Thermo Scientific) at days 9, 14, 21, and 28 after IRI. Transdermal FITC-sinistrin clearance was performed to measure glomerular filtration rate (GFR) in conscious mice 28 days after the initiation injury, as described.<sup>34</sup> FITC-sinistrin half-life was calculated using a 3-compartment model with linear fit using MPD Studio software (MediBeacon, Germany). All compound treatments were initiated 24 h after the initiating injury once a day for 7 days, and the investigator handling the mice and performing the assays (including histology) was blinded to treatment groups until all studies for that experiment were completed. PCI-34051 was solubilized in 10% Solutol HS, 20% PEG-400, and 70% water at pH 4.3, sonicated for 2 h at 60 °C, and administered by IP injection at 10 mg/kg and 50 mg/kg/day. All experimental protocols were approved by the Vanderbilt Institutional Animal Care and Use Committee.

**Analysis of Renal Fibrosis and Histone Acetylation.** To assess fibrosis, kidneys were harvested, fixed, and mounted in paraffin, and Sirius red staining and quantification were performed to evaluate renal fibrosis/collagen accumulation in the outer stripe of the outer medulla, as described.<sup>34</sup> Image capture and semiquantitative evaluation were performed by an observer blinded to treatment using ImageJ software. RNA isolation and quantitative RT-PCR were performed to evaluate expression of renal fibrosis markers in snap frozen kidneys using primer sequences and RNA extraction, as previously described.<sup>3</sup>

**Statistical Analyses.** Statistical analyses were performed using GraphPad Prism V9 (San Diego, CA), using Student's one-way ANOVA for multiple between-group comparisons. The minimal level of significance is indicated from pairwise comparisons and was set at  $p \leq 0.05$  for ANOVA studies. The  $p$  values shown were adjusted for multiple between group comparisons with false discovery rates of  $p < 0.05$  using the two-stage step up method of Benjamini, Krieger, and Yekutieli. Two-way ANOVA used to compare changes over time for BUN time course studies.

## ■ ASSOCIATED CONTENT

### SI Supporting Information

The Supporting Information is available free of charge at <https://pubs.acs.org/doi/10.1021/acspsci.1c00243>.

Table of physical properties; table of HDAC8 data; zfAKI data; compound 3 organoid data; human proximal tubule cell data for PCI-34051 and compound 1; PCI-34051 PK data; survival and BUN data for PCI-34051 in mouse AKI model; markers of renal fibrosis in mouse AKI model; synthetic protocols; <sup>1</sup>H and <sup>13</sup>C NMR spectra (PDF)

## ■ AUTHOR INFORMATION

### Corresponding Authors

**Donna M. Huryn** – Department of Pharmaceutical Sciences, School of Pharmacy, University of Pittsburgh, Pittsburgh, Pennsylvania 15261, United States; [orcid.org/0000-0001-5542-4968](https://orcid.org/0000-0001-5542-4968); Email: [huryn@pitt.edu](mailto:huryn@pitt.edu)

**Neil A. Hukriede** – Department of Developmental Biology, School of Medicine, University of Pittsburgh, Pittsburgh, Pennsylvania 15261, United States; [orcid.org/0000-0002-9655-9030](https://orcid.org/0000-0002-9655-9030); Email: [hukriede@pitt.edu](mailto:hukriede@pitt.edu)

### Authors

**Keith Long** – Department of Pharmaceutical Sciences, School of Pharmacy, University of Pittsburgh, Pittsburgh, Pennsylvania 15261, United States

**Zoe Vaughn** – Department of Pharmaceutical Sciences, School of Pharmacy, University of Pittsburgh, Pittsburgh, Pennsylvania 15261, United States

**Michael David McDaniels** – Department of Developmental Biology, School of Medicine, University of Pittsburgh, Pittsburgh, Pennsylvania 15261, United States; [orcid.org/0000-0002-7734-6072](https://orcid.org/0000-0002-7734-6072)

**Sipak Joyasawal** – Department of Pharmaceutical Sciences, School of Pharmacy, University of Pittsburgh, Pittsburgh, Pennsylvania 15261, United States; [orcid.org/0000-0001-6255-8833](https://orcid.org/0000-0001-6255-8833)

**Aneta Przepiorski** – Department of Developmental Biology, School of Medicine, University of Pittsburgh, Pittsburgh, Pennsylvania 15261, United States

**Emily Parasky** – Department of Developmental Biology, School of Medicine, University of Pittsburgh, Pittsburgh, Pennsylvania 15261, United States

**Veronika Sander** – Department of Molecular Medicine and Pathology, University of Auckland, Auckland, New Zealand 1010; [orcid.org/0000-0002-2918-833X](https://orcid.org/0000-0002-2918-833X)

**David Close** – Department of Pharmaceutical Sciences, School of Pharmacy, University of Pittsburgh, Pittsburgh, Pennsylvania 15261, United States

**Paul A. Johnston** – Department of Pharmaceutical Sciences, School of Pharmacy, University of Pittsburgh, Pittsburgh, Pennsylvania 15261, United States

**Alan J. Davidson** – Department of Molecular Medicine and Pathology, University of Auckland, Auckland, New Zealand 1010

**Mark de Caestecker** – Department of Medicine, Division of Nephrology, Vanderbilt University, Nashville, Tennessee 37235, United States

Complete contact information is available at: <https://pubs.acs.org/doi/10.1021/acspsci.1c00243>

### Author Contributions

The manuscript was written through contributions of all authors. All authors have given approval to the final version of the manuscript.

## Funding

The work was funded by DoD grant W81XWH-17-0610 and NIH grants 2R01 DK069403 and 2UC2 DK126122.

## Notes

The authors declare no competing financial interest.

## ACKNOWLEDGMENTS

We would like to thank Rachel Delgado for animal studies and Christopher Fitting, Prema Iyer, Jagannath Panda, and Sangeetha Subramani for synthesis of intermediates and resynthesis of standards. We are also grateful to Junmei Wang for computational studies related to assignment of absolute stereochemistry.

## ABBREVIATIONS

AKI, acute kidney injury; BUN, blood urea nitrogen; CCL, CC motif chemokine ligand; CHP, collagen hybridizing peptide; CKD, chronic kidney disease; clogP, calculated logarithm of partition coefficient; CXCL, CXC motif chemokine ligand; DAPI, 4',6-diamidino-2-phenylindole; dpf, days past fertilization; dpi, days past injection; FITC, fluorescein isothiocyanate; HDAC, histone deacetylase; HPRT1, hypoxanthine phosphoribosyltransferase 1; IL, interleukin; IRI, ischemia reperfusion-induced; IRI-AKI, ischemia reperfusion-induced acute kidney injury; NC, not calculated; NE, not effective; PK, pharmacokinetics; Q-RT-PCR, quantitative reverse transcription polymerase chain reaction; ROS, reactive oxygen species; SAHA, suberoylanilide hydroxamic acid; SERPINE1, serpine family E member 1; tGFR, transdermal glomerular filtration rate; THIQ, tetrahydroisoquinoline; TNF $\alpha$ , tumor necrosis factor alpha; TSA, trichostatin A; UUO, unilateral ureteral obstruction; zf, zebrafish

## REFERENCES

- (1) Kellum, J. A.; Romagnani, P.; Ashuntantang, G.; Ronco, C.; Zarbock, A.; Anders, H. J. Acute kidney injury. *Nat. Rev. Dis. Primers* **2021**, *7* (1), 52.
- (2) Nadim, M. K.; Forni, L. G.; Mehta, R. L.; Connor, M. J., Jr.; Liu, K. D.; Ostermann, M.; Rimmelé, T.; Zarbock, A.; Bell, S.; Bihorac, A.; Cantaluppi, V.; Hoste, E.; Husain-Syed, F.; Germain, M. J.; Goldstein, S. L.; Gupta, S.; Joannidis, M.; Kashani, K.; Koyner, J. L.; Legrand, M.; Lumlertgul, N.; Mohan, S.; Pannu, N.; Peng, Z.; Perez-Fernandez, X. L.; Pickkers, P.; Prowle, J.; Reis, T.; Srisawat, N.; Tolwani, A.; Vijayan, A.; Villa, G.; Yang, L.; Ronco, C.; Kellum, J. A. COVID-19-associated acute kidney injury: consensus report of the 25(th) Acute Disease Quality Initiative (ADQI) Workgroup. *Nat. Rev. Nephrol.* **2020**, *16* (12), 747–764.
- (3) Gameiro, J.; Marques, F.; Lopes, J. A. Long-term consequences of acute kidney injury: a narrative review. *Clin. Kidney J.* **2021**, *14* (3), 789–804.
- (4) Hulse, M.; Rosner, M. H. Drugs in development for acute kidney injury. *Drugs* **2019**, *79* (8), 811–82.
- (5) Chun, P. Therapeutic effects of histone deacetylase inhibitors on kidney disease. *Arch. Pharm. Res.* **2018**, *41*, 162–183.
- (6) Hyndman, K. A. Histone deacetylases in kidney physiology and acute kidney injury. *Semin. Nephrol.* **2020**, *40*, 138–147.
- (7) Levine, M. H.; Wang, Z.; Bhatti, T. R.; Wang, Y.; Aufhauser, D. D.; McNeal, S.; Liu, Y.; Cheraghlou, S.; Han, R.; Wang, L.; Hancock, W. W. Class-specific histone/protein deacetylase inhibition protects against renal ischemia reperfusion injury and fibrosis formation. *Am. J. Transplant* **2015**, *15* (4), 965–73.
- (8) Hyndman, K. A.; Kasztan, M.; Mendoza, L. D.; Monteiro-Pai, S. Dynamic changes in histone deacetylases following kidney ischemia-reperfusion injury are critical for promoting proximal tubule proliferation. *Am. J. Physiol. Renal Physiol.* **2019**, *316* (5), F875–F888.

(9) Tang, J.; Yan, Y.; Zhao, T. C.; Gong, R.; Bayliss, G.; Yan, H.; Zhuang, S. Class I HDAC activity is required for renal protection and regeneration after acute kidney injury. *Am. J. Physiol. Renal Physiol.* **2014**, *307*, F303–316.

(10) Zhang, Y.; Zou, J.; Tolbert, E.; Zhao, T. C.; Bayliss, G.; Zhuang, S. Identification of histone deacetylase 8 as a novel therapeutic target for renal fibrosis. *FASEB J.* **2020**, *34* (6), 7295–7310.

(11) Ha, S. D.; Solomon, O.; Akbari, M.; Sener, A.; Kim, S. O. Histone deacetylase 8 protects human proximal tubular epithelial cells from hypoxia-mimetic cobalt- and hypoxia/reoxygenation-induced mitochondrial fission and cytotoxicity. *Sci. Rep.* **2018**, *8* (1), 11332.

(12) Ho, T. C. S.; Chan, A. H. Y.; Ganesan, A. Thirty years of HDAC inhibitors: 2020 Insight and hindsight. *J. Med. Chem.* **2020**, *63* (21), 12460–12484.

(13) Banerjee, S.; Adhikari, N.; Amin, S. A.; Jha, T. Histone deacetylase 8 (HDAC8) and its inhibitors with selectivity to other isoforms: An overview. *Eur. J. Med. Chem.* **2019**, *164*, 214–240.

(14) Balasubramanian, S.; Ramos, J.; Luo, W.; Sirisawad, M.; Verner, E.; Buggy, J. J. A novel histone deacetylase 8 (HDAC8)-specific inhibitor PCI-34051 induces apoptosis in T-cell lymphomas. *Leukemia* **2008**, *22* (5), 1026–1034.

(15) Taha, T. Y.; Aboukhatwa, S.; Knopp, R.; Ikegaki, N.; Abdelkarim, H.; Neerasa, J.; Lu, Y.; Neelarapu, R.; Hanigan, T.; Thatcher, G.; Petukhov, P. Design, synthesis, and biological evaluation of tetrahydroisoquinoline-based histone deacetylase 8 selective inhibitors. *ACS Med. Chem. Lett.* **2017**, *8* (8), 824–829.

(16) Kovacic, P.; Edwards, C. L. Hydroxamic acids (therapeutics and mechanism): chemistry, acyl nitroso, nitroxyl, reactive oxygen species, and cell signaling. *J. Recept. Signal Transduct. Res.* **2011**, *31* (1), 10–9.

(17) Olson, D. E.; Sleiman, S. F.; Bourassa, M. W.; Wagner, F. F.; Gale, J. P.; Zhang, Y. L.; Ratan, R. R.; Holson, E. B. Hydroxamate-based histone deacetylase inhibitors can protect neurons from oxidative stress via a histone deacetylase-independent catalase-like mechanism. *Chem. Biol.* **2015**, *22* (4), 439–445.

(18) Whitehead, L.; Dobler, M. R.; Radetich, B.; Zhu, Y.; Atadja, P. W.; Claiborne, T.; Grob, J. E.; McRiner, A.; Pancost, M. R.; Patnaik, A.; Shao, W.; Shultz, M.; Tichkule, R.; Tommasi, R. A.; Vash, B.; Wang, P.; Stams, T. Human HDAC isoform selectivity achieved via exploitation of the acetate release channel with structurally unique small molecule inhibitors. *Bioorg. Med. Chem.* **2011**, *19* (15), 4626–34.

(19) Khan, N.; Jeffers, M.; Kumar, S.; Hackett, C.; Boldog, F.; Khramtsov, N.; Qian, X.; Mills, E.; Berghs, S. C.; Carey, N.; Finn, P. W.; Collins, L. S.; Tumber, A.; Ritchie, J. W.; Jensen, P. B.; Lichenstein, H. S.; Sehested, M. Determination of the class and isoform selectivity of small-molecule histone deacetylase inhibitors. *Biochem. J.* **2008**, *409* (2), 581–9.

(20) <https://bpsbioscience.com/fluorogenic-hdac8-assay-kit-50068>.

(21) Cianciolo Cosentino, C.; Skrypnik, N. I.; Brilli, L. L.; Chiba, T.; Novitskaya, T.; Woods, C.; West, J.; Korotchenko, V. N.; McDermott, L.; Day, B. W.; Davidson, A. J.; Harris, R. C.; de Caestecker, M. P.; Hukriede, N. A. Histone deacetylase inhibitor enhances recovery after AKI. *J. Am. Soc. Nephrol.* **2013**, *24* (6), 943–53.

(22) Chiba, T.; Skrypnik, N. I.; Skvarca, L. B.; Penchev, R.; Zhang, K. X.; Rochon, E. R.; Fall, J. L.; Pauksakon, P.; Yang, H.; Alford, C. E.; Roman, B. L.; Zhang, M. Z.; Harris, R.; Hukriede, N. A.; de Caestecker, M. P. Retinoic acid signaling coordinates macrophage-dependent injury and repair after AKI. *J. Am. Soc. Nephrol.* **2016**, *27* (2), 495–508.

(23) Kaplan, E. L.; Meier, P. Non-parametric estimation from incomplete observations. *J. Am. Stat. Assoc.* **1958**, *53*, 457–481.

(24) Long, K.; Kostman, S. J.; Fernandez, C.; Burnett, J. C.; Huryn, D. M. Do zebrafish obey Lipinski rules? *ACS Med. Chem. Lett.* **2019**, *10* (6), 1002–1006.

(25) Shultz, M. D. Two Decades under the influence of the rule of five and the changing properties of approved oral drugs. *J. Med. Chem.* **2019**, *62* (4), 1701–1714 and references cited therein.

(26) Liu, J.; Livingston, M. J.; Dong, G.; Tang, C.; Su, Y.; Wu, G.; Yin, X.-M.; Dong, Z. Histone deacetylase inhibitors protect against cis-platin-induced acute kidney injury by activating autophagy in proximal tubular cells. *Cell Death Dis.* **2018**, *9* (3), 322.

(27) Ryter, S. W.; Tyrrell, R. M. The heme synthesis and degradation pathways: role in oxidant sensitivity. Heme oxygenase has both pro- and antioxidant properties. *Free Radic Biol. Med.* **2000**, *28* (2), 289–309.

(28) Hwang, J.; Huang, Y.; Burwell, T. J.; Peterson, N. C.; Connor, J.; Weiss, S. J.; Yu, S. M.; Li, Y. In situ imaging of tissue remodeling with collagen hybridizing peptides. *ACS Nano* **2017**, *11* (10), 9825–9835.

(29) Perazella, M. A. Onco-nephrology: renal toxicities of chemotherapeutic agents. *Clin J. Am. Soc. Nephrol.* **2012**, *7* (10), 1713–21.

(30) Dasgupta, T.; Antony, J.; Braithwaite, A. W.; Horsfield, J. A. HDAC8 inhibition blocks SMC3 deacetylation and delays cell cycle progression without affecting cohesin-dependent transcription in MCF7 cancer cells. *J. Biol. Chem.* **2016**, *291* (24), 12761–12770.

(31) Novitskaya, T.; McDermott, L.; Zhang, K. X.; Chiba, T.; Pauksakon, P.; Hukriede, N. A.; de Caestecker, M. P. A PTBA small molecule enhances recovery and reduces postinjury fibrosis after aristolochic acid-induced kidney injury. *Am. J. Physiol Renal Physiol* **2014**, *306* (5), F496–504.

(32) Scarfe, L.; Menshikh, A.; Newton, E.; Zhu, Y.; Delgado, R.; Finney, C.; de Caestecker, M. P. Long-term outcomes in mouse models of ischemia-reperfusion-induced acute kidney injury. *Am. J. Physiol Renal Physiol.* **2019**, *317*, F1068–F1080.

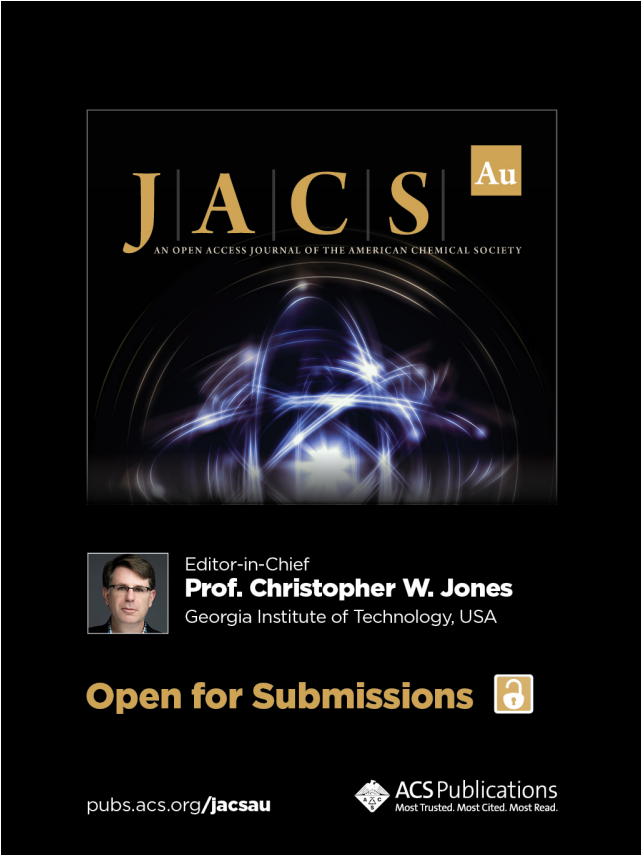
(33) Scarfe, L.; Schock-Kusch, D.; Ressel, L.; Friedemann, J.; Shulhevich, Y.; Murray, P.; Wilm, B.; de Caestecker, M. Transdermal measurement of glomerular filtration rate in mice. *J. Vis. Exp.* **2018**, *140*, e58520.

(34) Westerfield, M. *The zebrafish book. A guide for the laboratory use of zebrafish (Danio rerio)*, 4th ed.; University of Oregon Press: Eugene, 2000.

(35) Skrypnyk, N. I.; Sanker, S.; Skvarca, L. B.; Novitskaya, T.; Woods, C.; Chiba, T.; Patel, K.; Goldberg, N. D.; McDermott, L.; Vinson, P. N.; Calcutt, M. W.; Huryn, D. M.; Verneti, L. A.; Vogt, A.; Hukriede, N. A.; de Caestecker, M. P. Delayed treatment with PTBA analogs reduces postinjury renal fibrosis after kidney injury. *Am. J. Physiol Renal Physiol* **2016**, *310* (8), F705–F716.

(36) Przepiorski, A.; Sander, V.; Tran, T.; Hollywood, J. A.; Sorrenson, B.; Shih, J. H.; Wolvetang, E. J.; McMahon, A. P.; Holm, T. M.; Davidson, A. J. A simple bioreactor-based method to generate kidney organoids from pluripotent stem cells. *Stem Cell Reports* **2018**, *11* (2), 470–484.

(37) Przepiorski, A.; Crunk, A. E.; Holm, T. M.; Sander, V.; Davidson, A. J.; Hukriede, N. A. A simplified method for generating kidney organoids from human pluripotent stem cells. *J. Vis. Exp.* **2021**, DOI: 10.3791/62452.



**JACS Au**  
AN OPEN ACCESS JOURNAL OF THE AMERICAN CHEMICAL SOCIETY

Editor-in-Chief  
**Prof. Christopher W. Jones**  
Georgia Institute of Technology, USA

**Open for Submissions** 

pubs.acs.org/jacsau  ACS Publications  
Most Trusted. Most Cited. Most Read.